

Cation Interdiffusion in Polycrystalline Fluorite-cubic MgO-ZrO₂ Solid Solution

Yoshio SAKKA, Yasumichi OISHI,* and Ken ANDO

Department of Nuclear Engineering, Kyushu University, Higashi-ku Fukuoka 812

(Received July 24, 1981)

Lattice and grain-boundary interdiffusion coefficients were calculated from the concentration distributions as determined for cation interdiffusion in polycrystalline MgO-stabilized zirconias by applying a grain-boundary enhanced diffusion model. Lattice interdiffusion coefficients in the temperature range of 1650–1990 °C were represented by $\bar{D}=5.9 \times 10^{-4} \exp [-293(\text{kJ/mol})/RT] \text{ cm}^2/\text{s}$. Magnesium self-diffusion coefficients were calculated from the obtained interdiffusion coefficients and the reported Zr self-diffusion coefficients. The results confirmed that interdiffusion in the fluorite-cubic solid solution is primarily controlled by the diffusivity of the faster cation.

MgO-stabilized ZrO₂ (MSZ) is a fluorite-type cubic solid solution¹⁾ similar to CaO-stabilized ZrO₂ (CSZ). One difference is that the radius of the Mg ion is smaller than that of the Zr ion in MSZ, while that of the Ca ion is larger than that of the Zr ion in CSZ. Since MSZ exhibits high oxygen diffusivities similar to those of CSZ at high temperatures,²⁾ the defects in MSZ are assumed to be of the oxygen-vacancy type, as in CSZ.

During interdiffusion in oxygen-vacancy type fluorite structures, differing diffusivities of the two cations cause mass flow and electrical field effects on the cation interdiffusion, while the interchange of oxygen ions and oxygen vacancies on the simple cubic sublattice contributes only to the electrical field effect but does not necessarily contribute to the mass flow effect (since the concentration of the oxygen vacancy is equal to that of the dopant cation and therefore temperature-independent). For such conditions, an interdiffusion coefficient has been theoretically derived in terms of the self-diffusion coefficients of the constituent ions. The derived interdiffusion coefficient described satisfactorily interdiffusion in a CSZ system.³⁾ In the present work, a similar analysis was carried out for interdiffusion in the MSZ system to clarify the interdiffusion mechanism.

The self-diffusion coefficient of the oxygen ion in MSZ has been determined,²⁾ but that of the Mg ion has not. The tracer diffusion coefficient of the Zr ion in MSZ has not so far been determined but has been estimated from the Zr-Hf interdiffusion in the MgO-(Zr+Hf)O₂ system.⁴⁾ Since cation diffusion is enhanced by grain boundaries in polycrystalline CSZ,⁵⁾ a similar grain-boundary enhancement is assumed for the cations in polycrystalline MSZ.

In the present study, cation concentration distributions are determined after interdiffusion of polycrystalline diffusion couples, and lattice and grain-boundary interdiffusion coefficients are separately calculated. The results are compared with those of the CSZ system.⁶⁾

Experimental

Diffusion Couples and Diffusion Annealing. Appropriate mixtures of MgO (99.7% purity) and ZrO₂ (99.69% purity) to give the compositions of 12MgO·88ZrO₂, 16MgO·84ZrO₂, and 18MgO·82ZrO₂ were isostatically pressed into a pellet of 10 mm dia. and 10 mm height with the aid of dextrin

under a pressure of $6\text{--}7 \times 10^3 \text{ kg/cm}^2$. Pressed pellets were sintered in two ways: at 1750 °C for over 12 h in air, and at 2200 °C for 3 h in an Ar atmosphere. The densities of the sintered pellets ranged from 93–99% of the theoretical. The grain radii of the pellets, necessary to the present analysis, were determined using Fullman's relation.⁷⁾

Diffusion couples were prepared by joining pellets of different compositions at 1650 °C for 10 min in a molybdenum susceptor high-frequency induction furnace. Diffusion anneals were carried out at temperatures between 1650 and 1990 °C, where a single fluorite-cubic phase is stable according to the MgO-ZrO₂ phase diagram proposed by Grain.¹⁾ Diffusion anneals below 1730 °C were conducted in air using an SiC furnace, and those above 1823 °C using a tungsten-mesh heater furnace in an Ar atmosphere at 100 Torr. (1 Torr \approx 133.322 Pa).

Electron Probe Microanalysis. After diffusion annealing, each diffusion couple was sawed into halves parallel to the diffusion direction. One half was used for measuring the grain size to confirm that no grain growth occurred during diffusion annealing. The other half was employed for determining the concentration distribution by electron probe microanalysis. Mg and Zr distributions were determined at 20 μm intervals from the interface along the diffusion direction. Chemical compositions were determined from the relative intensities of the Mg K α and Zr L α_1 lines by using a calibration curve previously determined from standard samples.

Because of preferential diffusion of Mg and Zr ions along grain-boundaries, the Mg and Zr distributions perpendicular to the diffusion direction were not homogeneous in the present polycrystalline samples. Thus the composition at a given diffusion distance represents an average composition obtained by scanning perpendicular to the diffusion direction.⁴⁾

Results

The concentration distribution for grain-boundary enhanced diffusion has been described by Oishi and Ichimura as a function of the lattice and grain-boundary interdiffusion coefficients by,⁶⁾

$$\frac{2(C-C_1)}{C_2-C_1} = \frac{M_t}{M_\infty} \exp(-my), \quad (1)$$

where

$$\frac{M_t}{M_\infty} = 1 - \frac{6}{\pi^2} \sum_{n=1}^{\infty} \frac{1}{n^2} \exp\left(-\frac{\bar{D}n^2\pi^2t}{r^2}\right), \quad (2)$$

$$m = \left[\frac{4\bar{D}}{r\delta\bar{D}'} \sum_{n=1}^{\infty} \exp\left(-\frac{\bar{D}n^2\pi^2t}{r^2}\right) \right]^{1/2}, \quad (3)$$

y is the diffusion distance from the interface, C the

average concentration at y , C_1 and C_2 the initial concentrations of the diffusion couple, M_t and M_∞ the diffusion amounts at times t and infinity, respectively, \bar{D} and \bar{D}' the lattice and grain-boundary interdiffusion coefficients, respectively, r the grain radius, and δ the grain-boundary thickness.

Equation 1 can be rewritten as Eq. 4 in a logarithmic form,

$$\ln \frac{2(C-C_1)}{C_2-C_1} = \ln \frac{M_t}{M_\infty} - my, \quad (4)$$

showing that $\ln[2(C-C_1)/(C_2-C_1)]$ is proportional to the diffusion distance y .

An example of the MgO concentration distribution is shown in Fig. 1 for the diffusion couple of 12MgO·88ZrO₂ with 45 μ m grain radius and 16MgO·84ZrO₂,

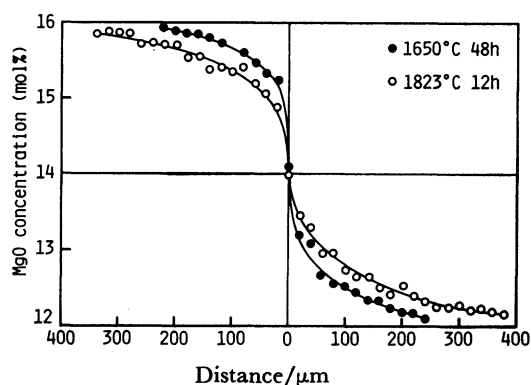


Fig. 1. Concentration distributions for the diffusion couples of 12MgO·88ZrO₂ and 16MgO·84ZrO₂.

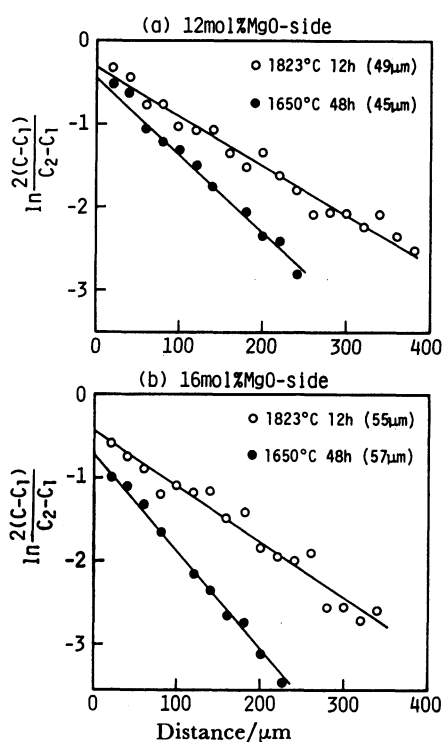


Fig. 2. Logarithmic concentration distributions for the diffusion couples of 12MgO·88ZrO₂ and 16MgO·84ZrO₂.

(a) 12 mol% MgO-side. (b) 16 mol% MgO-side.

with 57 μ m grain radius after annealing at 1650 °C for 48 h. Also shown is the MgO concentration for the diffusion couple of 12MgO·88ZrO₂ with 49 μ m grain radius and 16MgO·84ZrO₂ with 55 μ m grain radius after annealing at 1823 °C for 12 h. The corresponding $\ln[2(C-C_1)/(C_2-C_1)]$ values are plotted in Fig. 2 as a function of y , where the satisfactorily linear relationships indicate that the diffusion model represented by Eq. 1 is applicable to the present interdiffusion. The solid lines in Figs. 1 and 2 represent theoretical values calculated by Eq. 1 so as to provide the best fit to the experimental results. From the slopes and intercepts of the straight lines in Fig. 2, \bar{D} and $\delta\bar{D}'$ are separately calculated from Eqs. 2 and 3. A correction to diffusion time was made in all calculations for the period of joining the diffusion couple as well as for increasing and decreasing the temperature before and after an isothermal diffusion annealing.⁶⁾

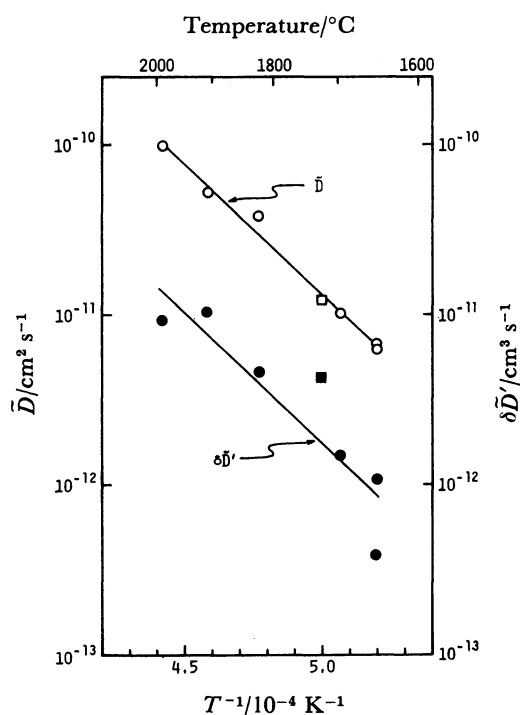


Fig. 3. Lattice interdiffusion coefficients and grain-boundary diffusion parameters for MSZ as a function of temperature. Circles denote the couple of 12MgO·88ZrO₂-16MgO·84ZrO₂ and squares the couple of 12MgO·88ZrO₂-18MgO·82ZrO₂.

The \bar{D} and $\delta\bar{D}'$ thus calculated are shown in Fig. 3, where the averages of values obtained on both sides of the diffusion couples are plotted. Circles denote the couple of 12MgO·88ZrO₂-16MgO·84ZrO₂ and squares the couple of 12MgO·88ZrO₂-18MgO·82ZrO₂. Comparison of \bar{D} for the two diffusion couples with different combinations of MgO contents indicates no significant composition dependence. Comparison of results from diffusion anneals conducted in air (below 1730 °C) and in an Ar atmosphere (above 1823 °C) indicates no noticeable effect of the atmosphere on the results.

Values of \bar{D} and $\delta\bar{D}'$ for the temperature range of

1650—1990 °C are described by Eqs. 5 and 6, respectively.

$$\tilde{D} = \left(5.9^{+5.8}_{-2.9}\right) \times 10^{-4} \exp[-293 \pm 11(\text{kJ/mol})/RT] \text{ cm}^2/\text{s}, \quad (5)$$

$$\delta\tilde{D}' = \left(1.0^{+5.1}_{-0.8}\right) \times 10^{-4} \exp[-279 \pm 30(\text{kJ/mol})/RT] \text{ cm}^3/\text{s}. \quad (6)$$

The activation energy for the grain-boundary diffusion parameter $\delta\tilde{D}'$ is close to that for lattice interdiffusion. Similar results have been also demonstrated for the CSZ system.⁶⁾

Discussion

The calculated \tilde{D} values are much smaller than the self-diffusion coefficients of the oxygen ion.²⁾

The relation between the interdiffusion coefficient and the self-diffusion coefficients of the constituent ions for the fluorite-cubic solid solution has been given by Eq. 7 as,³⁾

$$D = \frac{(Z_A^2 C_A C_B - Z_A Z_B C_A C_B + Z_0^2 C_B C_0) D_A D_0 + (Z_B^2 C_A C_B - Z_A Z_B C_A C_B + Z_0^2 C_A C_0) D_B D_0}{(Z_A^2 C_A C_B - Z_A Z_B C_A C_B) D_A + (Z_B^2 C_A C_B - Z_A Z_B C_A C_B) D_B + (Z_0^2 C_A C_0 + Z_0^2 C_B C_0) D_0}, \quad (7)$$

where Z is the valence, C the mole concentration, D the self-diffusion coefficient, and subscripts refer to the constituent ions. Since D_0 is much greater than D_{Zr} and D_{Mg} in the MSZ system, Eq. 7 reduces to Eq. 8.

$$D = [(Z_{Zr}^2 C_{Zr} C_{Mg} - Z_{Zr} Z_{Mg} C_{Zr} C_{Mg} + Z_0^2 C_{Mg} C_0) D_{Zr} + (Z_{Mg}^2 C_{Zr} C_{Mg} - Z_{Zr} Z_{Mg} C_{Zr} C_{Mg} + Z_0^2 C_{Zr} C_0) D_{Mg}] \times (Z_0^2 C_{Zr} C_0 + Z_0^2 C_{Mg} C_0)^{-1} \quad (8)$$

The Mg self-diffusion coefficients can be calculated by using Eq. 8 from known values of D and D_{Zr} . The Zr self-diffusion coefficients estimated for MSZ in the temperature range of 1680—2083 °C⁴⁾ have been represented by Eq. 9.

$$D_{Zr} = 0.033 \exp[-381(\text{kJ/mol})/RT] \text{ cm}^2/\text{s}. \quad (9)$$

The D_{Mg} values calculated by Eq. 8 from D_{Zr} (Eq. 9) and \tilde{D} (Eq. 5) for the average composition of the diffusion couple are represented by Eq. 10.

$$D_{Mg} = 3.7 \times 10^{-4} \exp[-285(\text{kJ/mol})/RT] \text{ cm}^2/\text{s}. \quad (10)$$

As shown in Fig. 4, the interdiffusion coefficient is higher in magnitude and lower in activation energy than D_{Zr} , and close to the calculated value of D_{Mg} both in magnitude and in activation energy. (The D_{Zr} in MSZ is similar to the D_{Zr} in CSZ in both magnitude and activation energy.⁴⁾)

The activation energy of D_{Mg} in MSZ (285 kJ/mol) is smaller than that of D_{Ca} in CSZ (419.2 kJ/mol).⁵⁾ This

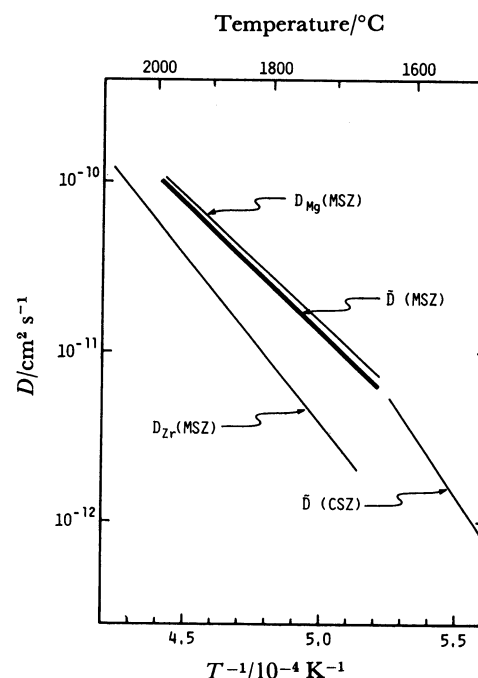


Fig. 4. Lattice interdiffusion coefficient and self-diffusion coefficients of Mg and Zr ions in MSZ; lattice interdiffusion coefficient in CSZ.⁶⁾

difference is interpreted as due to the ionic radii of the dopant cations relative to that of the Zr ion; that is, the Mg ion in MSZ is smaller than the Ca ion in CSZ.

Since D_R ($R = \text{Mg}$ or Ca) is greater than D_{Zr} in both MSZ and CSZ, \tilde{D} tends to be close to D_R in the respective systems in accordance with Eq. 7. Consequently, the small activation energy of interdiffusion in MSZ relative to that in CSZ, as shown in Fig. 4, is attributed to the activation energy of D_{Mg} in MSZ being smaller than that of D_{Ca} in CSZ.

In summary, cation interdiffusion in MgO-stabilized zirconia is controlled primarily by the diffusivity of the faster cation (Mg), and the contribution of the high diffusivity of the oxygen ion is small.

The authors acknowledge H. S. Spacil's comments to the manuscript.

References

- 1) C. F. Grain, *J. Am. Ceram. Soc.*, **50**, 288 (1967).
- 2) Y. Oishi, K. Ando, and M. Akiyama, *Nippon Kagaku Kaishi*, **1981**, 1445.
- 3) Y. Oishi and Y. Sakka, *J. Nucl. Mater.*, **97**, 44 (1981).
- 4) Y. Oishi, Y. Sakka, and K. Ando, *J. Nucl. Mater.*, **96**, 23 (1981).
- 5) W. H. Rhodes and R. E. Carter, *J. Am. Ceram. Soc.*, **49**, 244 (1966).
- 6) Y. Oishi and H. Ichimura, *J. Chem. Phys.*, **71**, 5134 (1979).
- 7) R. L. Fullman, *Trans. AIME*, **197**, 447 (1953).